Thrombomodulin Tightens the Thrombin Active Site Loops To Promote Protein C Activation†

Julia R. Koeppe,‡ Almagoul Seitova,§ Timothy Mather,§,|| and Elizabeth A. Komives*,‡

Department of Chemistry and Biochemistry, University of California at San Diego, La Jolla, California 92093-0378, Cardiovascular Biology Research Program, Oklahoma Medical Research Foundation, Oklahoma City, Oklahoma 73104, and Department of Biochemistry and Molecular Biology, University of Oklahoma Health Science Center, Oklahoma City, Oklahoma 73104

Received June 3, 2005; Revised Manuscript Received September 5, 2005

ABSTRACT: Thrombomodulin (TM) forms a 1:1 complex with thrombin. Whereas thrombin alone cleaves fibrinogen to make the fibrin clot, the thrombin−TM complex cleaves protein C to initiate the anticoagulant pathway. Crystallographic investigations of the complex between thrombin and TMEGF456 did not show any changes in the thrombin active site. Therefore, research has focused recently on how TM may provide a docking site for the protein C substrate. Previous work, however, showed that when the thrombin active site was occupied with substrate analogues labeled with fluorophores, the fluorophores responded differently to active (TMEGF1−6) versus inactive (TMEGF56) fragments of TM. To investigate this further, we have carried out amide H/^{2}H exchange experiments on thrombin in the presence of active (TMEGF45) and inactive (TMEGF56) fragments of TM. Both on-exchange and off-exchange experiments show changes in the thrombin active site loops, some of which are observed only when the active TM fragment is bound. These results are consistent with the previously observed fluorescence changes and point to a mechanism by which TM changes the thrombin substrate specificity in favor of protein C cleavage.

Thrombin is a dual-action protease in the blood clotting cascade acting as both a procoagulant (fibrinogen-cleaving) and an anticoagulant (protein C-cleaving). Thrombomodulin (TM)[1] by binding to thrombin inhibits the procoagulant activity of thrombin, and promotes the anticoagulant activity (*1*). TM contains six EGF-like domains, the fifth of which contains most of the thrombin-binding residues (*2*). Although the fifth domain is able to bind to thrombin and inhibit fibrinogen binding, the fourth domain increases binding affinity and is required for protein C activation. TMEGF45, containing both the fourth and the fifth EGF-like domains, is the smallest active cofactor fragment of TM (*3*). The sixth EGF-like domain also increases the affinity for thrombin compared to that of the fifth domain alone, but the TMEGF56 fragment does not give thrombin the ability to activate protein C (*4*).

The kinetics of binding of various inhibitors to thrombin are increased hundreds to thousands of times when TM is bound to thrombin (*5*−*9*). Protein C also binds to the TM−thrombin complex >1000-fold faster than to thrombin alone (*10*). The simplest explanation for why such a broad range of proteins exhibit altered rates of association is that TM alters the active site of thrombin, particularly the conformation of the loops surrounding the active site, to make association more favorable. These data are not easily reconciled with crystal structures of the thrombin−TMEGF456 complex versus thrombin alone, which show no differences in active site loops (*11*). Our hypothesis is that differences were not seen in the crystal structures because in all cases the active site was occupied by an inhibitor molecule and therefore the loops were already closed. Only a solution method such as amide proton exchange would be able to probe such subtle differences.

TM binds in anion-binding exosite (ABE1), a site on thrombin distal to the active site where fibrinogen and other cofactors also bind (*7*, *12*). Amide H/^{2}H exchange studies showed two surface loops on thrombin were protected from exchange when TMEGF45 bound: residues 54−61[2] (residues 33_{CT}−39_{CT}) and residues 93−109 (66_{CT}−81_{CT}) (*13*). These results agreed fully with the crystal structure of the thrombin−TMEGF456 complex (*11*) and with alanine scanning mutagenesis experiments (*10*, *14*, *15*).

In previous work, we observed changes in amide H/^{2}H exchange in several loops, including the ABE1 large loop

† Financial support for this work was provided by NIH Grant RO1−HL070999 to E.A.K.

* To whom correspondence should be addressed: Department of Chemistry and Biochemistry, University of California at San Diego, La Jolla, CA 92093-0378. Phone: (858) 534-3058. Fax: (858) 534-6174. E-mail: ekomives@ucsd.edu.

‡ University of California.

§ Oklahoma Medical Research Foundation.

|| University of Oklahoma Health Science Center.

[1] Abbreviations: TM, thrombomodulin; EGF, epidermal growth factor; PPACK, D-Phe-Pro-Arg-chloromethyl ketone; MALDI-TOF, matrix-assisted laser desorption time-of-flight.

[2] Thrombin residues are conventionally numbered according to an alignment with chymotrypsin, and this convention results in loop residues carrying numbers such as 60A, 60B, etc. This convention is confusing with amide-exchange data since information is lost regarding the length of the peptide fragment in which amide exchange is being assessed. We therefore will give all thrombin residue information as sequential numbers first, followed by the chymotrypsin convention numbers in parentheses with a subscripted CT to denote which are which.

10.1021/bi0510577 CCC: $30.25
Published on Web 10/21/2005

(residues 93−109, or 66_{CT}−81_{CT}) when PPACK is bound to the active site (*16*). On the basis of these results, we proposed two possible paths by which the active site communicates with ABE1. The first path involves $Leu40_{CT}$ in ABE1 which abuts the side chain of $Trp141_{CT}$ and $Gly193_{CT}$ at the back side of the active site (*17*). When TM binds at ABE1, it contacts the 33_{CT}−39_{CT} loop (*11*, *13*). Mutation of $Pro37_{CT}$ or $Gln38_{CT}$ to Ala weakens TM binding (*15*), and TM is thought to influence the position of $Glu39_{CT}$, relieving repulsion between this side chain and the incoming P3′ Asp of protein C (*18*). TM binding may also alter the conformation of the adjacent $Glu192_{CT}$, which when mutated to alanine converts the substrate specificity of thrombin toward protein C activation (*19*).

A second path of communication between ABE1 and the active site involves the contiguous strand extending from the TM binding site, residues 93−109 (66_{CT}−81_{CT}), to residues 117−132 ($90s_{CT}$ insertion loop). The $90s_{CT}$ loop is important for the Ca^{2+} dependence of protein C activation, and the triple mutant of $Arg93_{CT}$, $Arg97_{CT}$, and $Arg101_{CT}$ to Ala does not activate protein C (*20*, *21*). Single mutations of these arginines have been shown to affect TM binding and/or protein C activation (*14*, *15*). Crystal structures also show that the $90s_{CT}$ insertion loop helps to orient thrombin substrates in the active site (*22*, *23*).

To further investigate the thrombin−TM interaction, we used amide H/^{2}H exchange experiments to look for conformational differences within thrombin in the presence and absence of two different TM fragments: a cofactor-active TM fragment (TMEGF45) and a cofactor-inactive TM fragment (TMEGF56). These two fragments bind to thrombin with similar affinity at ABE1; however, only TMEGF45 promotes protein C activation. Thus, any differences in amide proton exchange elicited by only TMEGF45 and not by TMEGF56 may indicate changes that are important for the promotion of protein C activation. Our results show that TM binding causes conformational changes near the active site of thrombin, and that certain changes occur only upon binding of the cofactor-active TMEGF45 fragment but not upon binding of the cofactor-inactive TMEGF56 fragment.

EXPERIMENTAL PROCEDURES

Proteins. Bovine thrombin was purified from a barium citrate eluate (prepared from bovine plasma) according to previously published methods (*24*). The eluate powder (8 g) was redissolved overnight in 200 mL of 100 mM EDTA, and 150 mM NaCl, 10 mM sodium citrate, containing 11.1 g of ammonium sulfate and 0.03 g of benzamidine. Following resuspension, the concentration of ammonium sulfate was increased from 10 to 40%. After centrifugation at 10000*g*, the supernatant was kept, brought to 70% ammonium sulfate, and centrifuged. The pellet, containing prothrombin, was dissolved in 5 mL of 50 mM Tris (pH 7.5) and 150 mM NaCl and loaded onto a G-25 Sephadex gel filtration column (2.5 cm × 100 cm) to remove the ammonium sulfate, and the fraction containing the protein was collected. The prothrombin was activated by incubating it with 2.0 mg/mL *Echis carinatus* venom, 10 mM $CaCl_2$, and 1 mg/mL PEG-8000 for 45 min at 37 °C. The mixture was loaded onto a second G-25 Sephadex column (2.5 cm × 100 cm) equilibrated in 25 mM KH_2PO_4 (pH 6.5) and 100 mM NaCl, and the protein fraction was collected. Finally, the G-25 fraction containing active thrombin was loaded onto a MonoS FPLC 16/10 column (Amersham/GE Healthcare) equilibrated with buffer A [25 mM KH_2PO_4 (pH 6.5) and 100 mM NaCl]. The thrombin was eluted with a linear gradient of buffer B [25 mM KH_2PO_4 (pH 6.5) and 500 mM NaCl] over the course of 1 h. α-Thrombin was identified by fibrinogen clotting.

Human thrombin was obtained from purified prothrombin (Haematologic Technologies) as described previously (*16*). Optimal yields were obtained when the prothrombin concentrate was dissolved in 50 mM Tris (pH 7.5), 150 mM NaCl, 10 mM $CaCl_2$, and 1 mg/mL PEG-8000 so that the final prothrombin concentration was 1.6 mg/mL. The prothrombin was then activated for 2 h at 37 °C with 5 mg/mL *E. carinatus* venom, and purified as described above. α-Thrombin was identified by the fibrinogen clotting assay, and the protein concentration was determined by the absorbance at 280 nm ($\epsilon = 1.92$ cm mL unit^{-1} mg^{-1}).

For the mass spectrometry experiments, thrombin was buffer exchanged so that during the amide H/^{2}H exchange period the buffer would consist of 25 mM KH_2PO_4 (pH 6.5) and 50 mM NaCl. Human thrombin was exchanged into 12.5 mM KH_2PO_4 (pH 6.5) and 25 mM NaCl and concentrated to ∼1 mg/mL. Aliquots of 750 pmol of protein were lyophilized and stored at −80 °C until they were used.

TMEGF45 was expressed in *Pichia pastoris* yeast as described by White et al. (*3*). The protein was first purified by anion-exchange chromatography (QAE Sephadex followed by HiLoad 26/10 Q Sepharose) followed by HiLoad 16/60 Superdex 75 size-exclusion chromatography (Amersham/GE Healthcare). TMEGF45 was further purified and desalted by reverse-phase HPLC as described previously (*25*). TMEGF56 was prepared by expression in CHO cells as a fusion protein from an expression cassette derived from the RSV-PL4 vector (*26*) which contained the TMEGF56 fragment spanning residues 387−464 with a Met388Leu substitution and placed in a position C-terminal to the epitope tag for monoclonal antibody HPC-4. TMEGF56 was adsorbed from the cell media with HPC-4 immunoaffinity resin and purified by anion-exchange chromatography on Mono-Q resin (Amersham/GE Healthcare) as described previously (*26*). TMEGF56 was further purified by HiLoad 16/60 Superdex 75 size-exclusion chromatography (Amersham/GE Healthcare) and finally was exchanged into 12.5 mM KH_2PO_4 (pH 6.5) and 25 mM NaCl and concentrated to ∼5 mg/mL. Protein concentrations were determined by the BCA assay (Pierce Chemicals). After HPLC purification, portions of TMEGF45 (5625 pmol) were lyophilized out of H_2O and stored at −80 °C until they were used. TMEGF56 was stored lyophilized at −80 °C in portions containing 1875 pmol of protein.

Mass Spectrometry. Matrix-assisted laser desorption ionization time-of-flight (MALDI-TOF) mass spectra were acquired on a Voyager DE-STR instrument (Applied Biosystems) as previously described (*27*). The matrix used was 5.0 mg/mL α-cyano-4-hydroxycinnamic acid (Sigma-Aldrich) dissolved in a solution containing a 1:1:1 mixture of acetonitrile, ethanol, and 0.1% TFA. The pH of the matrix was adjusted to pH 2.2 using 2% TFA. The matrix solution was chilled on ice for at least 60 min prior to use, and the MALDI target plates were chilled overnight at 4 °C. Peptides

produced by pepsin cleavage of human and bovine thrombin were identified previously (*16*, *28*).

Amide H−^{2}H Exchange Experiments. The pH conditions during various stages of the reaction were determined on an Accumet Inlab 423 pH electrode (Mettler-Toledo) using nondeuterated mock solutions (to avoid having to recalibrate the electrode for deuterons). The number of deuterons incorporated into different regions of thrombin over the course of 10 min (on-exchange) was measured in buffered ^2H_2O [10 mM Tris base (pH 7.5)]. The kinetics of incorporation (on-exchange) are a good measure of the solvent accessibility of each region of thrombin. After incubation at 25 °C with 6 μL of H_2O to rehydrate the lyophilized thrombin, 30 μL of ^2H_2O was added to initiate on-exchange for times of 0.5−10 min. The samples were simultaneously quenched and diluted by addition of 120 μL of buffer (0 °C) with ∼10 μL of 2% TFA to give a final pH of 2.2. Each sample was then incubated with a 2-fold molar excess of immobilized pepsin (Pierce Chemicals) for 5 min at 4 °C. Pepsin beads were removed by centrifugation at 14 000 rpm for 10 s, and then the resulting thrombin peptide mixture was aportioned into several fractions, rapidly frozen in liquid N_2, and stored at −80 °C. On-exchange experiments were also performed on the thrombin−TMEGF45 and thrombin−TMEGF56 complexes. These experiments were performed in exactly the same manner as for thrombin alone, except that the TM fragment was dissolved in 6 μL of aqueous buffer [20 mM Tris base and 10 mM $CaCl_2$ (pH 8.5)] and added to the lyophilized thrombin so that the resulting pH of the mixture was 7.5 and everything was hydrated and mixed prior to addition of the 30 μL of ^2H_2O. The rest of the experiment proceeded in the same manner as for the thrombin alone.

The rates of off-exchange of deuterons from thrombin in complex with TM fragments were measured as described previously (*13*, *28*). Experiments were carried out at 25 °C. Lyophilized samples of either thrombin or TM were hydrated with 6 μL of ^2H_2O buffer. For experiments performed at pH 7.5, the thrombin buffer was 50 mM Tris base (pH 7.5), the TMEGF45 buffer was 20 mM Tris base and 10 mM $CaCl_2$ (pH 8.0), and the TMEGF56 buffer was 10 mM Tris base and 10 mM $CaCl_2$ (pH 8.0). For experiments performed at pH 8.0, the thrombin buffer was 50 mM Tris base (pH 8.0), the TMEGF45 buffer was 20 mM Tris base and 10 mM $CaCl_2$ (pH 8.0), and the TMEGF56 buffer was 10 mM Tris base and 10 mM $CaCl_2$ (pH 8.0). Thrombin and TM samples were incubated separately in ^2H_2O buffer for 8 min before they were combined (12 μL total volume) and allowed to form the complex for 2 min. The complex was off-exchanged for varying times (0 to 2 min) by 1:10 dilution into 120 μL of H_2O buffer [10 mM Tris base (pH 7.5 or 8.0, as appropriate)]. The pH variation of the complexation and dilution buffers was never more than ∼0.1 unit. H/^{2}H exchange was quenched at 0 °C to pH 2.2 by addition of 2% TFA (∼10 μL). The precise amount of TFA required for quenching was determined by titration prior to each experiment. Digestion of the quenched protein was carried out as described above. Pepsin beads were removed by centrifugation at 14 000 rpm for 10 s, and then the digest was aliquoted into several fractions, rapidly frozen in liquid N_2, and stored at −80 °C.

All samples were analyzed by MALDI-TOF mass spectrometry one at a time. Samples were rapidly thawed, mixed with cold matrix, spotted on a prechilled MALDI target plate, and dried under vacuum (*13*). The mass spectra were analyzed to determine the average number of deuterons present in each peptic peptide. The number of deuterons incorporated in each peptide was quantified by subtracting the centroid of the undeuterated control from the centroid of the isotopic peak cluster for the deuterated sample. All values reported represent only the deuterons exchanged onto the backbone amide−hydrogen (NH) positions. The residual deuterium content (5% for the on-exchange experiments and 4.5% for the off-exchange experiments) that was incorporated into rapidly exchanging side chain positions was subtracted. Finally, data were corrected for back-exchange loss (∼45%) as described previously (*16*). On-exchange was measured at 0, 0.5, 1, 2, 5, and 10 min, and the data were fit using a biexponential fit in Kaleidagraph as described previously (*29*). Off-exchange was measured at 0, 0.5, 1, and 2 min, and the data were fit using either a bi- or triexponential fit in Kaleidagraph as described previously (*13*).

RESULTS

Thrombin Conformational Dynamics Probed by Amide H−^{2}H Exchange. In previous work, we have shown that amide H/^{2}H exchange experiments followed by pepsin digestion and mass spectrometry can be used to probe the relative solvent accessibility of regions of thrombin to which different effector molecules are bound. In early work, the interface between thrombin and TMEGF45 was mapped using "off-exchange" experiments. In these experiments, the surface of the protein is first deuterated for 10 min and then the complex is formed and diluted into H_2O for varying times. The thrombin−TMEGF45 interface, which corresponded to ABE1, was found to have solvent-inaccessible amides when TMEGF45 was bound (*13*). During these studies, other changes in thrombin were observed that could not be readily explained. This led to the further probing of thrombin conformational dynamics using on-exchange experiments to compare PPACK-bound thrombin to the active site open form (*16*). In this latter work, we found that comparison of results from bovine and human thrombin could increase the degree of coverage of the thrombin sequence and help to verify some of the subtle effects that were observed. In the studies shown here, we used both on- and off-exchange experiments and also compared bovine and human thrombin to obtain the maximum certainty in the results. The pepsin fragments that are obtained from digestion of bovine and human thrombin cover approximately 50% of the thrombin sequence (Figure 1).

Thrombomodulin Binding at Anion Binding Exosite 1 (ABE1). ABE1 on thrombin is the binding site for both TM and fibrinogen. Two peptides present in the peptic digest of human thrombin covered ABE1. Residues 96−112 (65_{CT}−80_{CT}) are covered by a peptide with a mass MH^+ of 2127.19, and residues 97−117 (66_{CT}−84_{CT}) are covered by a peptide with a mass MH^+ of 2586.44. Only one peptide covered this region from bovine thrombin, and no further information was obtained in this case. Figure 2 shows that this region of thrombin incorporates deuterium quickly and is mostly deuterated by 10 min in the absence of TM. In the presence of TMEGF45 or TMEGF56, this region incorporates much

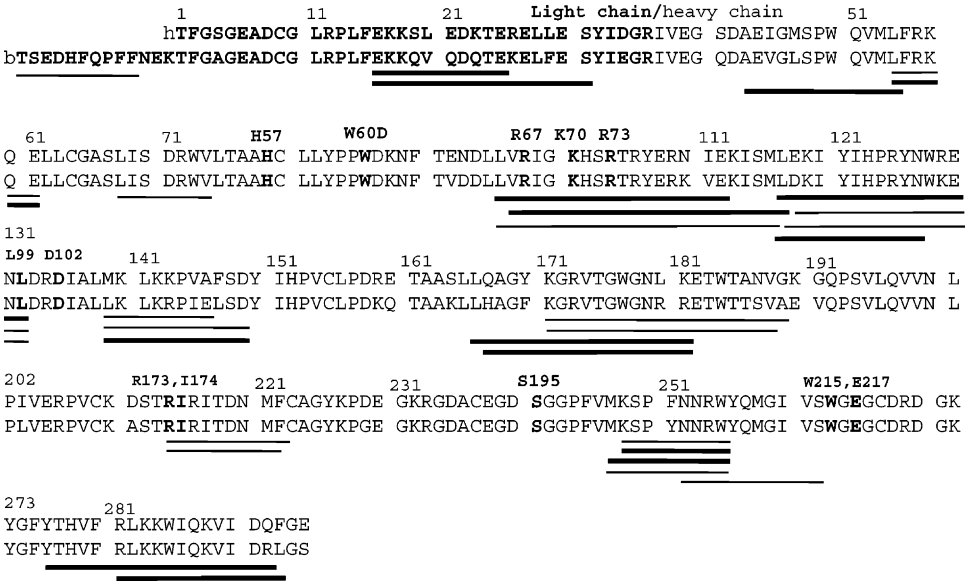

FIGURE 1: Aligned sequences of human and bovine α-thrombin showing all the peptides generated by pepsin cleavage as lines below the sequence. Thick lines denote peptides from the human protein digest, and thin lines denote those from the bovine digest. The light chain residues of thrombin are indicated with bold text, and significant residues, including the catalytic triad (H57, D102, and S195), are in both bold text and annotated above the sequence in the chymotrypsin numbering system. Coverage of the thrombin sequence is low, in part due to the four disulfide bonds present in thrombin.

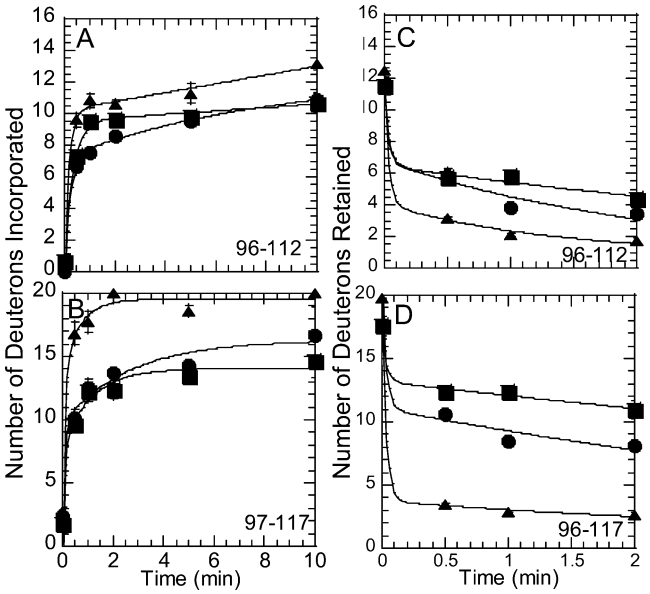

FIGURE 2: Amide H/^{2}H exchange at ABE1 of thrombin. (A) On-exchange into residues 96−112 (peptide with a mass MH^+ of 2127.19) of thrombin alone (▲), thrombin bound to TMEGF45 (●), and thrombin bound to TMEGF56 (■) at pH 7.5. (B) On-exchange into residues 97−117 (peptide with a mass MH^+ of 2586.44) of thrombin alone (▲), thrombin bound to TMEGF45 (●), and thrombin bound to TMEGF56 (■) at pH 7.5. (C) Off-exchange from residues 96−112 (peptide with a mass MH^+ of 2127.19) from thrombin alone (▲), thrombin bound to TMEGF45 (●), and thrombin bound to TMEGF56 (■) at pH 7.5. (D) Off-exchange from residues 97−117 (peptide with a mass MH^+ of 2586.44) from thrombin alone (▲), thrombin bound to TMEGF45 (●), and thrombin bound to TMEGF56 (■) at pH 7.5.

less deuterium, indicating that TM binding protects this surface loop from incorporation of deuterium into the solvent accessible amide positions. Also shown in Figure 2 (panels C and D) is a time course of deuterium off-exchange for these two peptides from thrombin alone and from thrombin bound to either TM fragment. When TM is absent, these peptides off-exchange nearly all of the incorporated deuterium by 2 min. When TM is bound to either TMEGF45 or TMEGF56, off-exchange is slower, and surface deuterons at amide positions are retained throughout the time course. In previous studies, we also reported protection of exchange of the thrombin surface loop containing residues 54−61 (residues 33_{CT}−39_{CT}) upon TM binding (*13*). Both TMEGF45 and TMEGF56 appeared to protect this loop equally as well in both bovine and human thrombin (data not shown). The H/^{2}H exchange results for these ABE1 peptides were the same at both pH 7.5 and 8.0, and the on-exchange and off-exchange results mirrored each other.

Exchange in the Autolysis Loop of Thrombin. Another site that differs in H/^{2}H exchange between TM-bound human thrombin and free human thrombin is the autolysis loop. This region of the protein is covered by a peptide with a mass MH^+ of 1506.78 (residues 167−180, or $Gln131_{CT}$−$Leu143_{CT}$). A much longer peptide covered this region from bovine thrombin which also extended into the core of thrombin so the shorter human thrombin peptide that only covers the loop is presented. On-exchange experiments show that this loop is less solvent accessible and only becomes partially deuterated in 10 min (Figure 3A). This region exhibited slower off-exchange in thrombin bound to either TM fragment (Figure 3B). This could be due to the proximity of W177 ($W141_{CT}$) in this loop to ABE1 that is in direct contact with TM. Similar results were seen at both pHs, but the effect was more dramatic at pH 8.0 perhaps because a somewhat higher level of deuteration was achieved.

TMEGF45 Affects Exchange of the 90s Loop in the Thrombin Active Site. The region of thrombin corresponding to the $90s_{CT}$ loop showed slowed H/^{2}H exchange only when thrombin was bound to TMEGF45. We first observed this effect in bovine thrombin in the peptide with a mass MH^+ of 2102.12 (residues 117−132, or $Leu84_{CT}$−$Leu99_{CT}$), which also extends around the thrombin molecule to ABE1. Figure 4A shows the mass spectra expanded around this peptide from the off-exchange experiments using bovine thrombin.

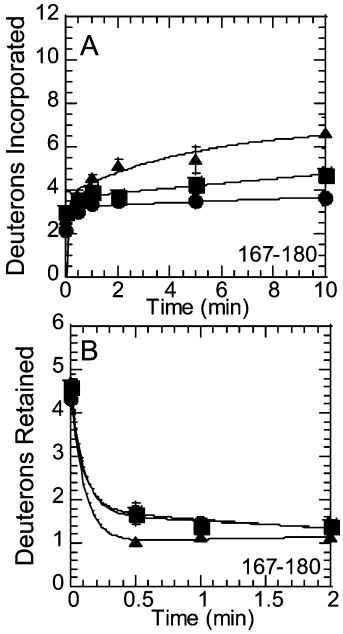

FIGURE 3: Amide H/^{2}H exchange at the autolysis loop of thrombin. (A) On-exchange into residues 167−180 (peptide with a mass MH^+ of 1506.78) of thrombin alone (▲), thrombin bound to TMEGF45 (●), and thrombin bound to TMEGF56 (■) at pH 7.5. (B) Off-exchange from residues 167−180 (peptide with a mass MH^+ of 1506.78) from thrombin alone (▲), thrombin bound to TMEGF45 (●), and thrombin bound to TMEGF56 (■) at pH 7.5.

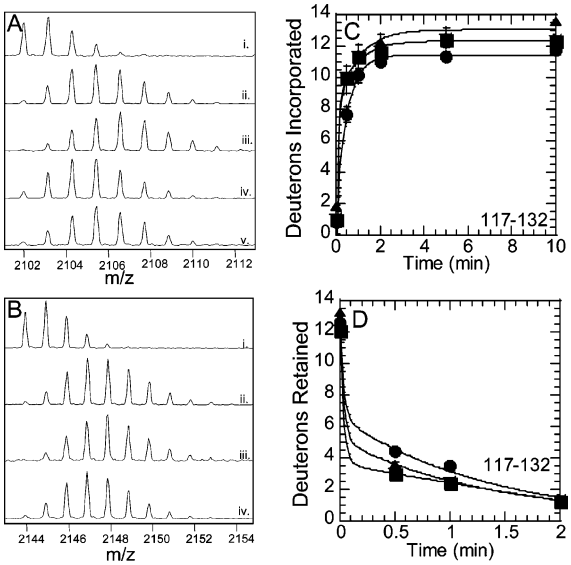

FIGURE 4: Amide H/^{2}H exchange at the 90s loop of thrombin. (A) Peptide mass envelope for the bovine thrombin peptide with a mass MH^+ of 2102.12 (i) before deuteration, (ii) after off-exchange for 0.5 min, (iii) after off-exchange for 0.5 min when bound to TMEGF45, (iv) after off-exchange for 1 min, and (v) after off-exchange for 1 min when bound to TMEGF45. (B) Peptide mass envelope for the human thrombin peptide with a mass MH^+ of 2144.14 (i) before deuteration, (ii) after off-exchange for 0.5 min, (iii) after off-exchange for 0.5 min when bound to TMEGF45, and (iv) after off-exchange for 0.5 min when bound to TMEGF56. (C) On-exchange into residues 117−132 (peptide with a mass MH^+ of 2144.14) of thrombin alone (▲), thrombin bound to TMEGF45 (●), and thrombin bound to TMEGF56 (■) at pH 7.5. (D) Off-exchange from residues 117−132 (peptide with a mass MH^+ of 2144.14) from thrombin alone (▲), thrombin bound to TMEGF45 (●), and thrombin bound to TMEGF56 (■) at pH 7.5.

After off-exchange for both 30 s and 1 min, deuterium retention is observed in this loop when TMEGF45 is bound

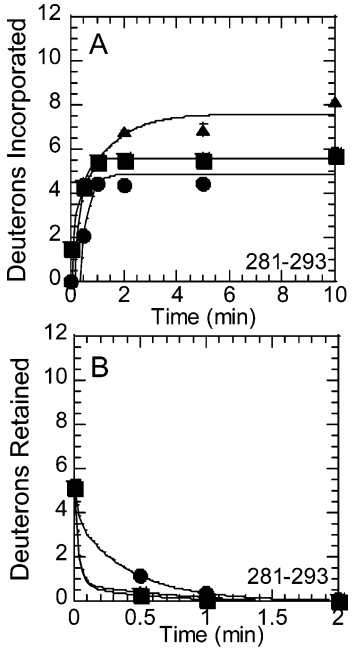

FIGURE 5: Amide H/^{2}H exchange at the C-terminus of thrombin. (A) On-exchange in a peptide with a mass MH^+ of 1702.02 of thrombin at pH 7.5. (B) Off-exchange in a peptide with a mass MH^+ of 1702.02 for free (▲), TMEGF45-bound (●), and TMEGF56-bound (■) thrombin.

(Figure 4A, traces iii and v) as compared to thrombin alone (Figure 4A, traces ii and iv). The loop was covered in human thrombin by the peptide with a mass MH^+ of 2144.14, which covered the same fragment, residues 117−132 ($Leu84_{CT}$−$Leu99_{CT}$). In this case, we compared off-exchange in the presence and absence of both TMEGF45 and TMEGF56. Only TMEGF45 slows the amide exchange in this region, and this can be seen from the raw data (Figure 4B) and from the kinetic plots (Figure 4C,D) for the peptide from human thrombin. A second peptide from human thrombin with a mass MH^+ of 1331.75, residues 117−126 ($Leu84_{CT}$−$Tyr94_{CT}$), ends before the $90s_{CT}$ loop but covers the adjacent segment that connects ABE1 to the $90s_{CT}$ loop. This shorter peptide could be analyzed only qualitatively because of complications of an overlapping higher-mass peptide peak. Even though the total amount of deuteration was not possible to determine, a small relative difference between free thrombin and TMEGF45-bound thrombin but not TMEGF56-bound thrombin could be observed (data not shown). For both peptides, the off-exchange rate was slower only when thrombin was bound to TMEGF45, although the difference was more pronounced in the peptide with a mass MH^+ of 2144.14. Again, these results were consistent at either pH, but the mass envelope of the shorter peptide (MH^+ of 1331.75) was better resolved at pH 8.0.

The C-Terminal Helix Is Also Tightened Only upon TMEGF45 Binding. The C-terminal helix of human thrombin was covered by a peptide with a mass MH^+ of 1702.02, residues 281−293 ($Arg233_{CT}$−$Phe245_{CT}$). This region exchanged more slowly, and differences in H/^{2}H on-exchange and off-exchange were seen only in the beginning of the time course (Figure 5). The mechanism by which TM alters the amide-exchange behavior of this helix is not readily explained from the structure but may be related to its proximity to the $90s_{CT}$ loop.

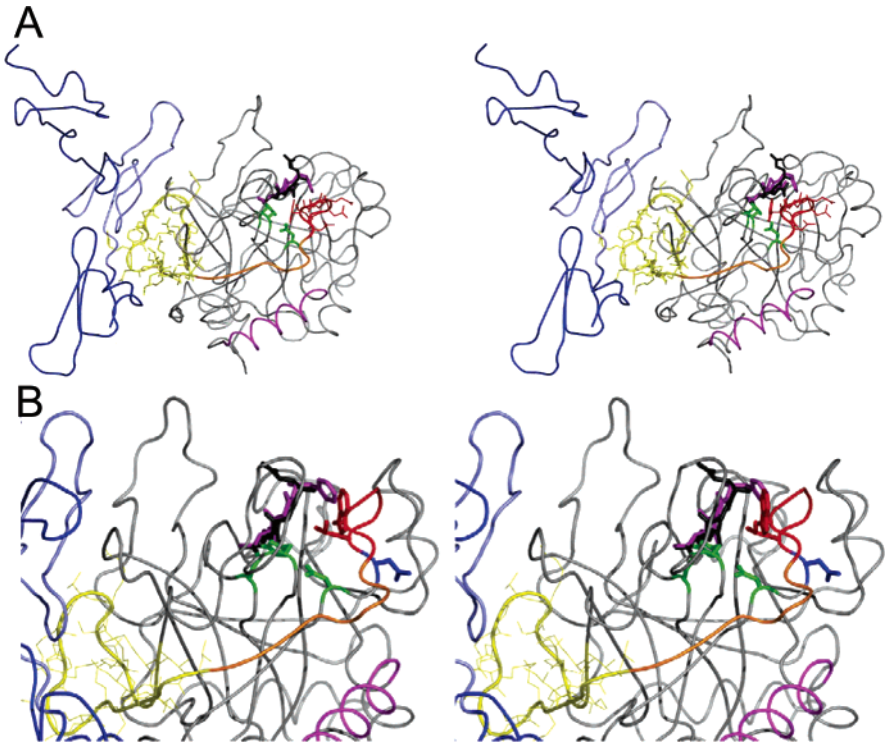

FIGURE 6: (A) Composite stereoview of the structure of PPACK thrombin (*17*) showing PPACK (purple) overlaid on the thrombin−TM complex (*11*) showing EGRCK in the active site (black). Only one thrombin backbone is shown (gray). TMEGF456 is colored blue. A surface strand (residues 117−126, 84_{CT}−94_{CT}, orange) connects the TM binding residues (residues 96−117, 65_{CT}−84_{CT}, yellow) and results in conformational change in the $90s_{CT}$ loop (residues 126−132, 94_{CT}−99_{CT}, red). This strand abuts the C-terminal helix (residues 281−293, $Arg233_{CT}$−$Phe245_{CT}$, magenta) which also shows decreased solvent accessibility upon TMEGF45 binding. (B) Close-up stereoview of the active site of the same figure as in panel A. The P3 Phe from the PPACK inhibitor (purple) is seen interacting with Trp96 and Leu99 in the $90s_{CT}$ loop (red), while the P3 Glu from the EGRCK inhibitor (black) is seen pointing away from Asp100 (blue) and Asp102 (green).

DISCUSSION

Mechanism of TM Communication from ABE1 to the Active Site. One of the fascinating features of thrombin is the many loops that surround its active site. Our results showed that in both bovine and human thrombin, binding of TM at ABE1 directly affects the conformational ensemble of at least two of these loops (the $140s_{CT}$ loop and the $90s_{CT}$ loop). The $140s_{CT}$ loop exhibited a decreased solvent accessibility when either TMEGF45 or TMEGF56 bound.

In both bovine and human thrombin, decreased solvent accessibility was observed at the $90s_{CT}$ loop when TMEGF45 was bound. The extent of amide proton exchange can be decreased due to direct protein binding, to increased secondary structure content, or to changes in the conformational ensemble (i.e., dynamics changes). Because the decreased solvent accessibility was observed in a loop on the surface of thrombin that is not near the TM binding site, it is most likely due to changes in the conformational ensemble. The decrease in solvent accessibility may be attributed to a "tightening" of the conformational ensemble of the $90s_{CT}$ loop. The coverage of the human thrombin sequence by pepsin digestion gave three peptides that revealed the pathway from ABE1 where TM binds to the active site where changes were observed (Figure 6A). This allows us to postulate a mechanism in which TM binding at ABE1 (residues 96−117, or 65_{CT}−84_{CT}) effectively pulls on the connecting strand (residues 117−126, or 84_{CT}−94_{CT}) and alters the conformation of the $90s_{CT}$ loop (residues 126−132, or 94_{CT}−99_{CT}). Remarkably, this long-distance tightening of the $90s_{CT}$ loop was only observed when TMEGF45 was bound and not when TMEGF56 was bound despite the fact that the binding sites and affinities of these two different TM fragments are very similar. Thus, the fourth domain of TM must be responsible for causing changes at the active site of thrombin. Other work has shown that the fourth domain of TM alters the structure and dynamics of the fifth domain (*30*, *31*), and it is therefore not unreasonable to postulate that it could alter the way the fifth domain interacts with thrombin.

Comparison with Results from Active Site Fluorescent Labels. In experiments performed by Ye et al., dansyl fluoride attached to the active site serine showed changes in fluorescence when thrombin bound TM (*32*). For this label, the fluorescence shifted in the presence of both the active cofactor (TMEGF1−6) and the inactive cofactor (TMEGF56) even though TMEGF56 does not confer protein C cleavage activity. When instead fluorescein-FPR or ANS-FPR was attached to the active site histidine, the FPR linkage positioned the fluorophore farther from the active site serine. Interestingly, this fluorescent label responded specifically to TM(1−6) and not to TMEGF56 (*33*). However, because it was not known where the fluorophore was exactly positioned in the active site, it was not possible to identify a specific site on thrombin that was being affected by TM(1−6) and not TMEGF56 binding (*33*).

The fluorescence results strongly correlate with our amide $H/^2H$ exchange results. Either TMEGF45 or TMEGF56 caused reduced exchange in the $140s_{CT}$ loop that is at the back of the active site near $Ser195_{CT}$. But only TMEGF45, the smallest active fragment of TM, caused reduced rate of

Table 1: Amino Acid Alignment for Naturally Occurring Substrates of Thrombin[a]

substrate	P6	P5	P4	P3	P2	P1	P1′	P2′	P3′	P4′
fibrinogen										
human (Aα)	Glu	Gly	Gly	Gly	Val	Arg	Gly	Pro	Arg	Val
bovine (Aα)	Glu	Gly	Gly	Gly	Val	Arg	Gly	Pro	Arg	Val
human (B*β*)	Gly	Phe	Phe	Ser	Ala	Arg	Gly	His	Arg	Pro
PPACK				Phe	Pro	Arg				
protein C										
human	Asp	Gln	Val	**Asp**	Pro	Arg	Leu	Ile	**Asp**	Gly
bovine	Asp	Gln	Leu	**Asp**	Pro	Arg	Ile	Val	**Asp**	Gly
protein C CK				Glu	Gly	Arg				
inhibitor	**P6**	**P5**	**P4**	**P3**	**P2**	**P1**	**P1′**	**P2′**	**P3′**	**P4′**
antithrombin III										
human	Val	Val	Ile	Ala	Gly	Arg	Ser	Leu	Asn	Pro
bovine	Val	Val	Ile	Ala	Gly	Arg	Ser	Leu	Asn	Ser
protein C inhibitor										
human	Thr	Ile	Phe	Thr	**Phe**	Arg	Ser	Ala	Arg	Leu

[a] Sequences were obtained from searching the gene databank at NCBI and from the CRC publication edited by Machovich (*34*). P*x* denotes the number of positions by which the residue precedes the P1 Arg. P*x*′ denotes the number of positions by which the residue follows the P1 Arg. The two repulsive P3 and P3′ Asp residues in the protein C substrate are in bold.

exchange in the $90s_{CT}$ loop and the C-terminal helix, which form the binding site for the P2 and P3 residues. One might ask whether conformational differences are seen in this loop when the structure of PPACK-bound thrombin is compared to that of EGRCK-bound thrombin, and the answer is no (*11*). However, the Phe at the P3 position of PPACK is indeed interacting with $Leu99_{CT}$ and $Trp101_{CT}$, while the Glu at the P3 position of EGRCK points away from the $90s_{CT}$ loop, presumably repelled by $Asp100_{CT}$ and $Asp102_{CT}$ (Figure 6B).

Substrate Specificity Changes that Would Result from Alteration of the 90s$_{CT}$ Loop. TM is undoubtedly promoting protein C activation by several mechanisms, none of which are mutually exclusive. A wealth of kinetic data indicate that TM alters the active site that is "seen" by approaching substrates and inhibitors. BPTI binding kinetics are specifically enhanced by TM fragments containing the fourth domain (*6*, *8*, *9*). Association of the protein C inhibitor with the thrombin−TM complex is accelerated 140-fold compared with the rate for thrombin alone (*5*). The protein C inhibitor has a Phe at the P2 position, which is normally occupied by a small side chain (Table 1). Protein C also associates 1000-fold faster with the thrombin−TM complex than with thrombin alone (*10*). TM may open or twist the $90s_{CT}$ loop, improving access to the active site and resulting in the observed dramatic increase in association rates for these varied substrates and inhibitors.

One way TM may promote the association of thrombin with its alternative substrate protein C is to relieve electrostatic repulsion between protein C and the active site of thrombin. Site-directed mutagenesis studies have suggested that TM removes the electrostatic repulsion between $Glu39_{CT}$ and the P3′ Asp of protein C and the electrostatic repulsion from $Glu192_{CT}$ at the base of the active site (*18*, *19*). Neither of these sites is contacted directly by TM (*10*); however, we observed that both TMEGF45 and TMEGF56 induce amide-exchange differences near these residues.

The amide H/^{2}H exchange experiments uniquely point to a role for the $90s_{CT}$ loop in optimal substrate recognition at the P3 position of protein C. Only the cofactor-active TMEGF45, which is able to promote protein C activation, causes tightening of the $90s_{CT}$ loop. Protein C has an Asp at the P3 position, whereas fibrinogen has a Phe. TM-induced alteration of the $90s_{CT}$ loop could remove electrostatic repulsion between $Asp100_{CT}$ and $Asp102_{CT}$ of thrombin and the P3 Asp of protein C, thus improving its approach to the active site of thrombin. Also, only the cofactor-active TMEGF45 caused reduced exchange in the C-terminal helix which abuts the $90s_{CT}$ loop. $Asp100_{CT}$ is hydrogen bonded to $Ser214_{CT}$, so it is likely that alteration of the $90s_{CT}$ loop also will affect the conformation of the $220s_{CT}$ loop. Although we do not have peptide coverage of the $220s_{CT}$ loop in the amide-exchange studies, alanine scanning experiments have suggested that residues in this loop are also important for protein C recognition (*10*).

The amide H/^{2}H exchange experiments presented here give direct evidence that TM causes subtle changes in thrombin; however, the crystal structure of thrombin bound to TMEGF456 showed no differences in thrombin compared with PPACK-inactivated thrombin (*11*). There are several plausible explanations for this discrepancy. One possibility is that the complex seen in the crystals already has the active site loops closed, perhaps because there is a covalent substrate at the active site. Indeed, loop repositioning prior to binding may be assessed best by association kinetic experiments, which show dramatic differences between free thrombin and TM-bound thrombin (*10*). A second possibility is that TM may cause alterations in the dynamic ensemble of thrombin that cannot be observed in the crystals. Such subtle conformational or dynamic changes can perhaps best be observed by amide H/^{2}H exchange experiments such as those presented here. Amide H/^{2}H exchange is a new experimental tool that reveals, in the most direct way so far achieved, the subtle changes that occur only when a cofactor-active TM fragment is bound. They also reveal the pathway within the thrombin molecule by which changes are transmitted from the TM binding site to the active site.

ACKNOWLEDGMENT

J.R.K. acknowledges support from the Cell and Molecular Genetics Training Program.

REFERENCES

1. Esmon, C. T. (2000) Regulation of blood coagulation, *Biochim. Biophys. Acta 1477*, 349−360.
2. Srinivasan, J., Hu, S., Hrabal, R., Zhu, Y., Komives, E. A., and Ni, F. (1994) Thrombin-bound structure of an EGF subdomain from human thrombomodulin determined by transferred nuclear Overhauser effects, *Biochemistry 33*, 13553−13560.
3. White, C. E., Hunter, M. J., Meininger, D. P., White, L. R., and Komives, E. A. (1995) Large-scale expression, purification and characterization of small fragments of thrombomodulin: The roles of the sixth domain and of methionine 388, *Protein Eng. 8*, 1177−1187.
4. Kurosawa, S., Stearns, D. J., Jackson, K. W., and Esmon, C. T. (1988) A 10-kDa cyanogen bromide fragment from the epidermal growth factor homology domain of rabbit thrombomodulin contains the primary thrombin binding site, *J. Biol. Chem. 263*, 5993−5996.
5. Rezaie, A. R., Cooper, S. T., Church, F. C., and Esmon, C. T. (1995) Protein C inhibitor is a potent inhibitor of the thrombin-thrombomodulin complex, *J. Biol. Chem. 270*, 25336−25339.
6. Rezaie, A. R., He, X., and Esmon, C. T. (1998) Thrombomodulin increases the rate of thrombin inhibition by BPTI, *Biochemistry 37*, 693−699.

7. Myles, T., Church, F., Whinna, H., Monard, D., and Stone, S. R. (1998) Role of thrombin anion-binding exosite-I in the formation of thrombin-serpin complexes, *J. Biol. Chem. 273*, 31203−31208.
8. De Cristofaro, R., and Landolfi, R. (1999) Allosteric modulation of BPTI interaction with human α- and ζ-thrombin, *Eur. J. Biochem. 260*, 97−102.
9. van de Locht, A., Bode, W., Huber, R., Le Bonniec, B. F., Stone, S. R., Esmon, C. T., and Stubbs, M. T. (1997) The thrombin E192Q-BPTI complex reveals gross structural rearrangements: Implications for the interaction with antithrombin and thrombomodulin, *EMBO J. 16*, 2977−2984.
10. Xu, H., Bush, L. A., Pineda, A. O., Caccia, S., and Di Cera, E. (2005) Thrombomodulin changes the molecular surface of interaction and the rate of complex formation between thrombin and protein C, *J. Biol. Chem. 280*, 7956−7961.
11. Fuentes-Prior, P., Iwanaga, Y., Huber, R., Pagila, R., Rumennik, G., Seto, M., Morser, J., Light, D. R., and Bode, W. (2000) Structural basis for the anticoagulant activity of the thrombin-thrombomodulin complex, *Nature 404*, 518−525.
12. Ayala, Y. M., Cantwell, A. M., Rose, T., Bush, L. A., Arosio, D., and Di Cera, E. (2001) Molecular Mapping of Thrombin-Receptor Interactions, *Proteins: Struct., Funct., Genet. 45*, 107−116.
13. Mandell, J. G., Baerga-Ortiz, A., Akashi, S., Takio, K., and Komives, E. A. (2001) Solvent accessibility of the thrombin-thrombomodulin interface, *J. Mol. Biol. 306*, 575−589.
14. Nagashima, M., Lundh, E., Leonard, J. C., Morser, J., and Parkinson, J. F. (1993) Alanine-scanning mutagenesis of the epidermal growth factor-like domains of human thrombomodulin identifies critical residues for its cofactor activity, *J. Biol. Chem. 268*, 2888−2892.
15. Pineda, A. O., Cantwell, A. M., Bush, L. A., Rose, T., and Di Cera, E. (2002) The thrombin epitope recognizing thrombomodulin is a highly cooperative hot spot in exosite I, *J. Biol. Chem. 277*, 32015−32019.
16. Croy, C. H., Koeppe, J. R., Bergqvist, S., and Komives, E. A. (2004) Allosteric Changes in Solvent Accessibility Observed in Thrombin upon Active Site Occupation, *Biochemistry 43*, 5246−5255.
17. Bode, W., Turk, D., and Karshikov, A. (1992) The refined 1.9-Å X-ray crystal structure of D-Phe-Pro-Arg chloromethylketone-inhibited human α-thrombin: Structure analysis, overall structure, electrostatic properties, detailed active-site geometry, and structure−function relationships, *Protein Sci. 1*, 426−471.
18. Le Bonniec, B. F., MacGillivray, R. T., and Esmon, C. T. (1991) Thrombin Glu-39 restricts the P′3 specificity to nonacidic residues, *J. Biol. Chem. 266*, 13796−13803.
19. Le Bonniec, B., and Esmon, C. (1991) Glu-192→Gln substitution in thrombin mimics the catalytic switch induced by thrombomodulin, *Proc. Natl. Acad. Sci. U.S.A. 88*, 7371−7375.
20. Ye, J., Rezaie, A. R., and Esmon, C. T. (1994) Glycosaminoglycan contributions to both protein C activation and thrombin inhibition involve a common arginine-rich site in thrombin that includes residues arginine 93, 97, and 101, *J. Biol. Chem. 269*, 17965−17970.
21. He, X., Ye, J., Esmon, C. T., and Rezaie, A. R. (1997) Influence of Arginines 93, 97, and 101 of thrombin to its functional specificity, *Biochemistry 36*, 8969−8976.
22. Stubbs, M. T., Oschkinat, H., Mayr, I., Huber, R., Angliker, H., Stone, S. R., and Bode, W. (1992) The interaction of thrombin with fibrinogen. A structural basis for its specificity, *Eur. J. Biochem. 206*, 187−195.
23. Martin, P. D., Robertson, W., Turk, D., Huber, R., Bode, W., and Edwards, B. F. (1992) The structure of residues 7−16 of the A α-chain of human fibrinogen bound to bovine thrombin at 2.3-Å resolution, *J. Biol. Chem. 267*, 7911−7920.
24. Ni, F., Konishi, Y., and Scheraga, H. A. (1990) Thrombin-bound conformation of the C-terminal fragments of hirudin determined by transferred nuclear Overhauser effects, *Biochemistry 29*, 4479−4489.
25. Wood, M. J., and Komives, E. A. (1999) Production of large quantities of isotopically labeled protein in *Pichia pastoris* by fermentation, *J. Biomol. NMR 13*, 149−159.
26. Rezaie, A. R., and Esmon, C. T. (1992) The function of calcium in protein C activation by thrombin and the thrombin-thrombomodulin complex can be distinguished by mutational analysis of protein C derivatives, *J. Biol. Chem. 267*, 26104−26109.
27. Mandell, J. G., Falick, A. M., and Komives, E. A. (1998) Measurement of amide hydrogen exchange by MALDI-TOF mass spectrometry, *Anal. Chem. 70*, 3987−3995.
28. Mandell, J. G., Falick, A. M., and Komives, E. A. (1998) Identification of protein−protein interfaces by decreased amide proton solvent accessibility, *Proc. Natl. Acad. Sci. U.S.A. 95*, 14705−14710.
29. Hughes, C. A., Mandell, J. G., Anand, G. S., Stock, A. M., and Komives, E. A. (2001) Phosphorylation causes subtle changes in solvent accessibility at the interdomain interface of methylesterase CheB, *J. Mol. Biol. 307*, 967−976.
30. Wood, M. J., Sampoli-Benitez, B. A., and Komives, E. A. (2000) Solution structure of the smallest cofactor-active fragment of thrombomodulin, *Nat. Struct. Biol. 7*, 200−204.
31. Prieto, J. H., Sampoli Benitez, B. A., Melacini, G., Johnson, D. A., Wood, M. A., and Komives, E. A. (2005) Dynamics of the fragment of thrombomodulin containing the fourth and fifth EGF-like domains correlate with function, *Biochemistry 44*, 1225−1233.
32. Ye, J., Esmon, N. L., Esmon, C. T., and Johnson, A. E. (1991) The active site of thrombin is altered upon binding to thrombomodulin. Two distinct structural changes are detected by fluorescence, but only one correlates with protein C activation, *J. Biol. Chem. 266*, 23016−23021.
33. Ye, J., Liu, L. W., Esmon, C. T., and Johnson, A. E. (1992) The 5th and 6th Growth Factor-Like Domains of Thrombomodulin Bind to the Anion-Binding Exosite of Thrombin and Alter Its Specificity, *J. Biol. Chem. 267*, 11023−11028.
34. Machovich, R. (1984) in *The Thrombins*, pp 166, CRC Press, Boca Raton, FL.

BI0510577